ISSN 0001-4338, Izvestiya, Atmospheric and Oceanic Physics, 2009, Vol. 45, No. 3, pp. 372–379. © Pleiades Publishing, Ltd., 2009.
Original Russian Text © S.A. Kitaigorodskii, 2009, published in Izvestiya AN. Fizika Atmosfery i Okeana, 2009, Vol. 45, No. 3, pp. 399–407.

# Determining the Influence of Wind-Wave Breaking on the Dissipation of the Turbulent Kinetic Energy in the Upper Ocean and on the Dependence of the Turbulent Kinetic Energy on the Stage of Wind-Wave Development

**S. A. Kitaigorodskii**

*Department of Earth and Planetary Seiences, the Johns Hopkins University, Baltimore, Maryland 21218-2687*

*e-mail: sergei.kitaigorodskii@luukku.com*

Received January 23, 2006; in final form, March 22, 2006

**Abstract**—New experimental data that make it possible to explain and predict the observed variability of turbulent-energy dissipation in the upper ocean are discussed. For this purpose, the dependence of the energy dissipation rate of breaking wind waves on their propagation velocity (see [1]) is used. The turbulent-energy dissipation values obtained earlier in [2, 3] by a direct method are compared to the results of radar measurements of individual breaking events presented in [1]. On the basis of this comparison, a strong dependence of the turbulent-energy dissipation value on the stage of wind-wave development, which is characterized by the ratio $U_a/c_p$ ($U_a$ is the wind speed and $c_p$ is the phase speed of the peak of the wind-wave spectrum) is confirmed. This dependence was found earlier purely empirically. Moreover, it is shown that the theoretically obtained dependence $\left(\frac{c_p}{U_a}\right)^4$, does not contradict the available empirical data. The results of this study opens possibilities for scientifically substantiated calculations of greenhouse-gas exchange (specifically, $CO_2$ exchange between the ocean and the atmosphere).

**DOI:** 10.1134/S0001433809030104

## 1. INTRODUCTION

The schemes used in [3–5] to describe physical processes of ocean–atmosphere local interaction are based only on the characteristics of atmospheric and oceanic turbulence and wind waves that are determined via direct methods, i.e., on the basis of the most perfect present-day techniques of measuring different statistical characteristics of oceanic turbulence and wind waves. This relates primarily to such difficultly determined characteristics as the turbulent-energy dissipation immediately beneath breaking waves, $\varepsilon_0$; the width of the dissipation subrange in the wave spectrum, which is characterized by the quantity $\omega_g$, which represents the low-frequency boundary of this subrange; and the values of aerodynamic roughness of the ocean surface as seen from both above ($z_0$) and below ($z_{od}$), which are determined from measurements of the quantity $\omega_g$ and the entire wind-wave spectrum. With this approach, a certain dependence of these quantities on the stage of wind-wave development has been established in most cases. This stage is characterized by the quantity $U_a/c_p$ (where $U_a$ is the wind speed and $c_p$ is the phase speed of the spectral peak.

This study shows the efficiency of this approach by using different methods of determining $\varepsilon_0$—the value of turbulent kinetic energy dissipation immediately beneath breaking waves.

## 2. CONCLUSIONS OF THE THEORY OF THREE-DIMENSIONAL TURBULENCE FOR THE UPPER OCEAN SUBJECTED TO WIND WAVES

The most constructive way of determining the variability of turbulent-energy dissipation $\varepsilon_t$ in the upper ocean is the use of the theory developed in [5, 6], according to which the system of determining parameters for describing the variability of $\varepsilon_i$, can be written as

$$\varepsilon_t = f(u_{*w}, z, K_0, z_{od}), \quad z > 0, \tag{1}$$

where $u_{*w}$ is the friction velocity in the upper ocean; $z$ is depth; $K_0$ is a constant (in depth) turbulent viscosity, which is defined by analogy with shear-free turbulence; and $z_{od}$ is the parameter of ocean surface roughness as seen from below, which may be described, in accordance with [12], by the following formula:

$$z_{od} = 0.1K_0/u_* \text{ для } \mathrm{Re}_s = \frac{K_0}{\nu} \gg 1. \tag{2}$$

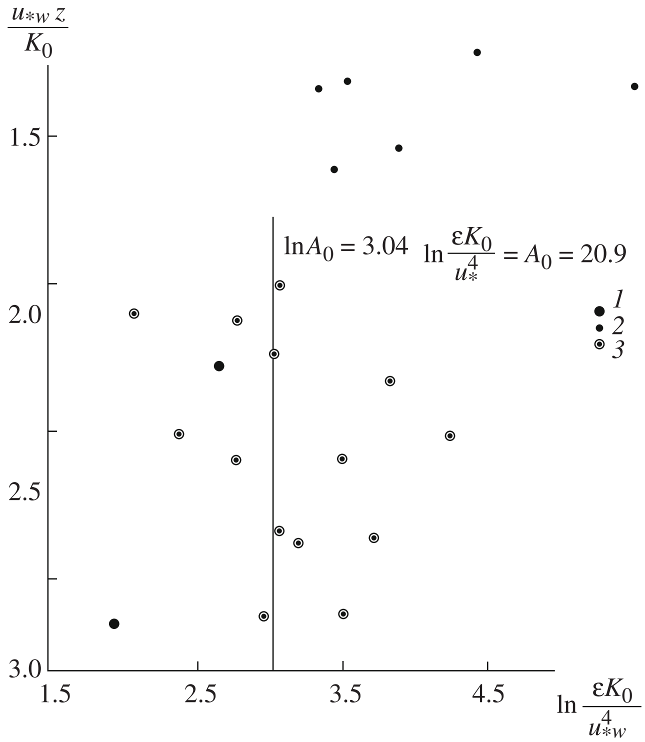


**Fig. 1.** Universal function $\frac{\varepsilon_0 K_0}{u_{*w}^4} = F\left(\frac{u_{*w}z}{K_0}\right)$ for the SWADE experiment [3]. The average value of $\frac{\varepsilon_0 K_0}{u_{*w}^4} = A_0$ in the region with dissipation presumably constant in depth is determined and shown in this figure as $\ln A_0 = 3.04$; six points, which are indicative of a rapid decrease of $\varepsilon_t$ with $z$ in the range $1.6 > \frac{u_{*w}z}{K_0} > 1.2$, are also shown: (*1*) two values from the WAVES experiment [3], *2*) SWADE data in the region $\varepsilon(z)$, and (*3*) SWADE data in the region $\varepsilon_t = \text{const} = \varepsilon_0$.

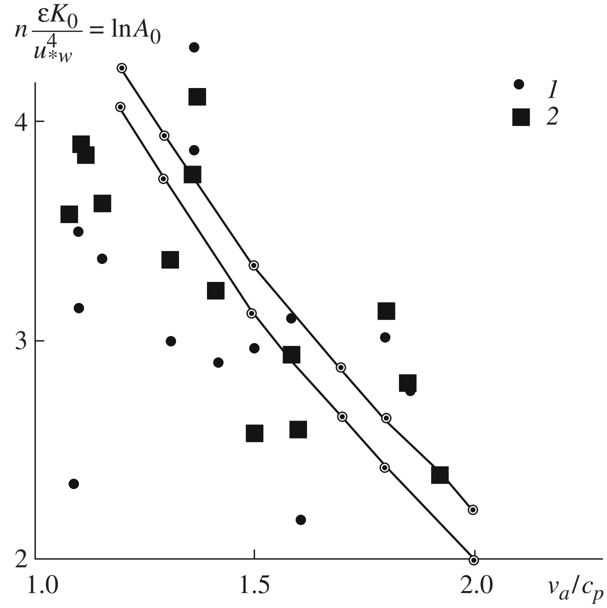


**Fig. 2.** Variation of dissipation in the surface layer [4] with the inverse wind-wave age $\frac{U_a}{c_p}$ from the SWADE data. The dissipation values are shown that are determined from the data on fluctuations in the (*2*) horizontal and (*1*) vertical velocity components. The curves correspond to $A_0 = 150\left(\frac{U_a}{c_p}\right)^{-4}$ and $A_0 = 122\left(\frac{U_a}{c_p}\right)^{-4}$, respectively.

In view of (2) and according to [6], it is possible to assume that

$$\varepsilon_i = \frac{u_{*w}^4}{K_0} F\left(\frac{u_{*w}z}{K_0}\right) \text{ для } z > z_{od}. \quad (3)$$

The latter formula shows that the rate of turbulent-energy dissipation $\varepsilon_t$ depends on both the characteristics of the velocity-shear flow (through the quantity $u_{*w}$) and the turbulent-energy diffusion flux, which predominates in the case of shear-free turbulence (by means of the quantity $K_0$). In the region of turbulent patches that form as a result of different types of wind-wave breaking, or, more precisely, in the region $\frac{u_{*w}z}{K_0} \le O(1)$ $\left(\frac{z}{z_{od}} \le 10\right)$ in (3), it was assumed that the dissipation $\varepsilon_t$ is already independent of $z$, so that $\varepsilon_t = \varepsilon_t(u_{*w}, K_0)$, or

$$F = A_0; \quad \varepsilon_t = \varepsilon_0 = A_0 \frac{u_{*w}^4}{K_0}, \quad (4)$$

where $A_0$ is a dimensionless constant coefficient.

It is formula (4) that is the most constructive result of [3, 5], which indicates that, in the course of generation of turbulence under the wind effect in the presence of wave breaking, the dissipation value $\varepsilon_0$ may depend on both the velocity shear (through $u_{*w}$) and the turbulent-energy flux, which is directed deep from the center of the patches generated by the process of wave breaking (through $K_0$). In [3], much attention was given to both the possible existence of a noticeable depth range where (4) is valid and the determination of the values of the constant $A_0$ for different conditions of coexistence of waves and wind, i.e., at different stages of wave growth. It has been found (see Fig. 2c in [3]) that, for the initial stages of wave development (a very small wind fetch and a rapid growth of

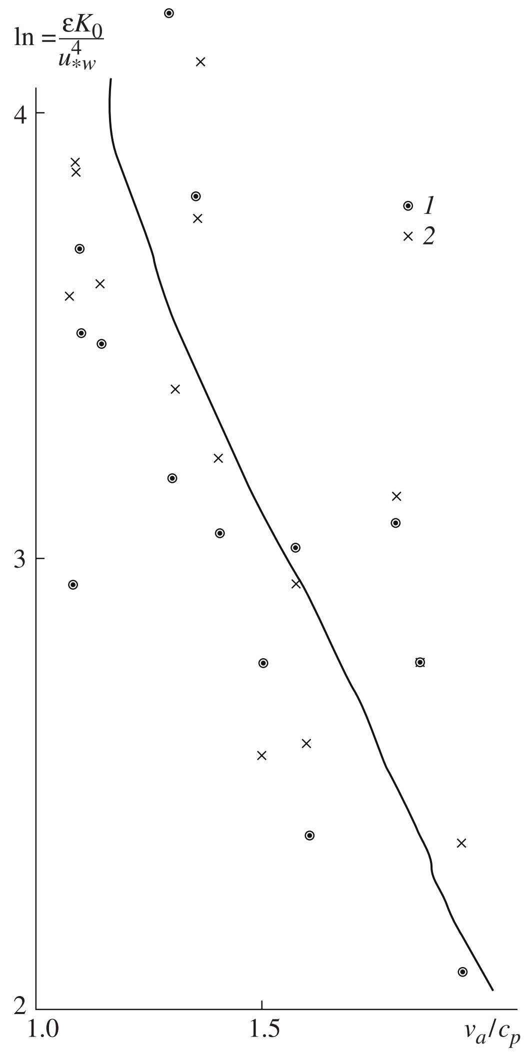


**Fig. 3.** Turbulent-energy dissipation values that are obtained for different values of the inverse wind-wave age $\frac{U_a}{c_p}$, from (*2*) the horizontal velocity components and (*1*) the values of $\ln\left(\frac{\varepsilon_u K_0}{u_{*w}^4} + \frac{\varepsilon_w K_0}{u_{*w}^4}\right)$. Curve (*1*) corresponds to $A_0 = 122\left(\frac{U_a}{c_p}\right)^{-4}$.

waves; $\left(\frac{c_p}{u_{*a}} \approx 4\text{–}8;\ \frac{U_a}{c_p} \approx 0.13\text{–}0.26\right)$ 0.13–0.26, where $u_{*a}$ is the friction velocity in the near-water atmospheric layer), the depth range in which (4) is valid could not been detected in [3] (on the other hand, the region was revealed in which $\varepsilon_t \sim z^{-2}$ for both stable and unstable stratification). At the same time, this depth range was observed to a depth of $\frac{u_{*w}z}{K_0} \le 3.0$ for the SWADE experimental data [7], which corresponded to developed wind waves$\left(\frac{U_a}{c_p} \approx 1.0\text{–}2.0\right)$ in the open ocean. The average value of $A_0$ obtained from these data was 20.9 (see Fig. 6c in [3]). This value was found without allowance for the values of $\varepsilon_t(z)$ in a thin surface layer, where variations in $\varepsilon_t(z)$ with depth were observed.

Analyzing the SWADE data in [2], I was able to obtain a rough estimate for the variability of $A_0$ depending on the age of wind waves $U_a/c_p$:

$$A_0(1) = 320;\quad A_0(1.3) = 120;\quad A_0(1.5) = 90;\quad A_0(2) = 60 \tag{5}$$

where the average value is $A_0 = 140$. These data were presented in my report at the International Symposium on Gas Exchange in Miami in 2000. In contrast to the aforementioned average value $A_0 = 20.9$, these data were obtained without the initial selection of experimental data for the region where $\varepsilon_t(z) = \text{const}$, which is reason for different average values of $A_0$ (20–140). Now, it is possible to give a more complete description of $A_0$ variability both theoretically and experimentally. This issue is considered in the following sections.

## 3. PARAMETRIZATION OF THE PROCESS OF WAVE-ENERGY DISSIPATION DUE TO WAVE BREAKING AND THE USE OF THIS PARAMETRIZATION FOR DETERMINING THE DISSIPATION OF TURBULENT KINETIC ENERGY IN THE SURFACE OCEAN LAYER

On the basis of radar measurements, an effort was first made in [1] to immediately determine the dependence of the energy dissipation rate in breaking wind waves on their propagation velocity. For this purpose, measurements of individual breaking events were used. In most cases, the connection between the lifetime of a surf ($\tau_e$) and the speed of its motion ($C_e$) was clearly defined. The details of this experiment are more thoroughly described in our study [5] as well. Our main interest here is the wave-energy dissipation as a function of $C_e$ (or the wave number $k_e = g/C_e^2$). Searching for such dependences is commonly based on the following initial relation for the wave-energy dissipation per unit length of wave crests $\varepsilon_L$:

$$\varepsilon_L = b\rho_w g^{-1} C_e^5, \tag{6}$$

where $\rho_w$ is the density of water and $g$ is the acceleration of gravity. This relation was found in laboratory experiments performed above quasi-stationary break-

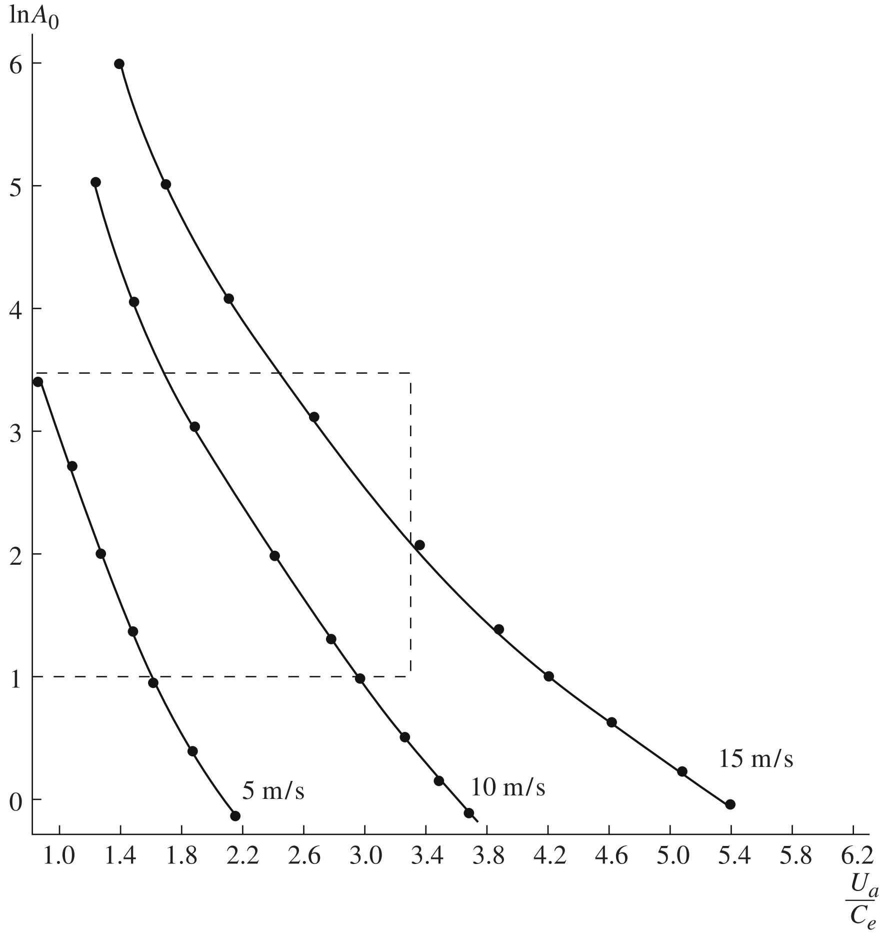


**Fig. 4.** Dependence of $\ln A_0$ (23) on $U_a/C_e$ for different wind speeds $U_a$ (m/s). The square shows the region of the observed values of $\ln A_0$ according to Figs. 1–3.

ing waves. The values of the numerical coefficient $b$ in (6) can be chosen using the relation

$$b = \pi\frac{\delta}{\lambda_e}, \quad (7)$$

which was derived in [5]. In (7), $\delta$ is the characteristic vertical size of the jet (its thickness) that forms in the course of breaking and moves forward with the speed $C_e$ in the direction of motion of the surf and $\lambda_e = \frac{2\pi C_e^2}{g}$ is the wavelength of the breaking wave, which is substantially greater than $\delta$, so that $b$ is a small numerical coefficient. Its value is estimated at 0.03 in [9]. The range of its values for different types of breaking waves $b = (3–16) \times 10^{-3}$ is given in [10]. For the wave-energy dissipation value per unit area $\varepsilon_S$, it is possible to use the expression

$$\varepsilon_S \approx b\frac{\rho_w C_e^5}{g\lambda_e}. \quad (8)$$

In [1], the emphasis was on determining the dependence of the wave-energy dissipation on the quantity $C_e$. With this goal, in his study [1], Phillips introduced the function $\Lambda(C_e)$ to characterize the length of breaking elements (surfs). It does not have the dimension of length, because it represents the average length per unit area and unit speed range, i.e., a dimension of $[\Lambda(C_e)] = \frac{T}{L^2}$. The methods of determining the quantity $\Lambda(C_e)$ are more thoroughly described in [5]. Using this quantity, the authors of [1] considered the quantity

$$\varepsilon_w(C_e) = \frac{\varepsilon_S}{\Delta C_e} = b\rho_w g^{-1} C_e^5 \Lambda(C_e) \quad (9)$$

as a function of the speed of breaking-front motion $C_e$ (or the speed of surf motion). This dependence is depicted in Fig. 6 from [5], where the distribution of $\frac{\varepsilon_w(C_e)}{b}$ is shown. It is this quantity that is of primary importance for our purposes, because it gives the distribution (over $C_e$, $k_e$, or $\lambda_e$) of the wave energy that is lost during wave breaking per unit volume. Under certain conditions, this distribution can be compared to the turbulent-energy dissipation value in turbulent patches that form beneath the sea surface as a result of wave breaking. More accurately, the expression for $\varepsilon_w(C_e)$ may be written as

$$\varepsilon_w(C_e) = b\alpha\rho_w g^{-1} C_e^5 \Lambda(C_e), \tag{10}$$

where $\alpha$ is a numerical coefficient, which characterizes the ratio of the average length of a turbulent patch that forms during wave breaking to the quantity $C_e\tau_e$ ($\tau_e$ is the average lifetime of the patch (or surf)). The value of $\alpha$ must be within the range 0.5–1.0 [5]. In order to find the relation between the wave-energy dissipation value per unit volume $\varepsilon_w$ and the turbulent-energy dissipation value per unit mass in turbulent patches that arise from wind-wave breaking, it is necessary to know the lifetime of surges (i.e., individual breaking elements, or the so-called breaking events). In [1], a sufficiently reliable relation was established between the average lifetime of a surf $\tau_e$ and its speed $C_e$. This relation may be written as [1]

$$\tau_e = 5\frac{C_e}{g} = \frac{5}{2\pi}\tau = 0.8\tau, \tag{11}$$

where $\tau = \frac{2\pi}{(gk)^{1/2}} = \frac{2\pi}{g}C$ is the wave period. Then, the expression for the turbulent-energy dissipation $\varepsilon_0$ per unit mass in turbulent patches that are formed by surfs may be written as

$$\varepsilon_0 = \frac{\varepsilon_w(C_e)}{\rho_w\tau_e} = \frac{b\alpha}{5}C_e^4\Lambda(C_e). \tag{12}$$

Equating (4) and (12), we obtain the following desired expression for the constant $A_0$ in formula (4) for $\varepsilon_0$:

$$A_0 = \frac{b\alpha}{5}\left(\frac{C_e}{u_{*w}}\right)^4 \Lambda(C_e)K_0. \tag{13}$$

This expression will be subjected to further analysis and used for numerical estimations and comparison with the data on $A_0$ variability obtained earlier in [5]. To conclude this section, we notice that a strong increase in $A_0$ with the inverse wind-wave age $\left(\frac{C_e}{U_a}\right)$, which was found in [2, 3], is completely supported by formula (13).

## 4. NUMERICAL ESTIMATES FOR $A_0$

When formula (13) is used, the emphasis should be on determining the range of possible variations in the quantity $\Lambda(C_e)$ and the coefficient of turbulent viscosity (constant in depth) $K_0$, which can also depend on $C_e$ (more precisely, on the ratio $\frac{C_e}{u_{*w}}$). However, under the existing uncertainty in choosing many quantities that are used to parametrize the processes under study, it is necessary to take into account the fact that many of these quantities can be determined only to within an order of magnitude. We start with the coefficient $K_0$. The theory developed by the author [11, 12] has led to the following result:

$$K_0 = a_{br}^2\omega_g = 2\omega_g\int_{\omega_g}^{\omega} S(\omega)d\omega, \tag{14}$$

where $a_{br}$ is the rms amplitude of breaking waves and $\omega_g$ is the low-frequency limit of the dissipation range in the frequency spectrum of waves, which characterizes the frequency of breaking waves. If

$$S(\omega) = \beta g^2\omega^{-5} \quad \omega \ge \omega_g, \tag{15}$$

$$K_0 = \frac{\beta}{2}g^2\omega_g^{-3}, \tag{16}$$

where $\beta = 0.025$ is the Phillips constant. In view of recent data [5, 13], when $K_0$ is estimated in (18), the possible dependence of $\omega_g$ on the stage of wave development, i.e., on the ratio $C_e/u_{*w}$ in this context, should be taken into account (see Fig. 8 in [5]). If the typical average value $\frac{\omega_g U_a}{g} = 4.0$ is immediately taken for the quantity $\omega_g U_a/g$, then according to (16), we find that

$$K_0 = 2\times 10^{-4}\frac{U_a^3}{g}. \tag{17}$$

So, even for such small wind speeds as 5 m/s, formula (17) leads to $K_0 = 20$ cm$^2$/s; i.e., it gives a value of the same order of magnitude as viscosity in the shear layer, where it is on the order of $u_{*w}h$ if $h \approx 50$ cm, i.e., on the order of $a_{br}$. Analysis of the WAVES and SWADE experimental data in [3] has shown that that the corresponding value of $\omega_g U_a/g$ is in the range 5.0–12.0. In [4], it was assumed that $\frac{\omega_g U_a}{g} = 6.0$ (see Fig. 3 in [4]), which is most typical of conditions close to developed wind waves. Below, we will take $\frac{\omega_g U_a}{g} = 5.0$, which leads to

$$K_0 = 1.0 \times 10^{-4} \frac{U_a^3}{g}, \tag{18}$$

because value (18) was chosen by us earlier in [3] during analysis of the SWADE experiment [3]. As is seen, calculations of $K_0$ turn out to be rather sensitive to the values chosen for $\frac{\omega_g U_a}{g}$. It is likely that the actual variability of the quantity $\frac{K_0 g}{U_a^3}$ can be estimated at $(0.5–2.0) \times 10^{-4}$, depending on the value chosen for $\frac{\omega_g U_a}{g}$. (The data of [3] that are presented below for the SWADE experiment [3] were also obtained at $\omega_g U_a/g \approx 5.0$, so that their use here does not require any recalculations.) As for the quantity $\Lambda(C_e)$, its values are given in Fig. 5 from [5] and, according to [1], lie in the range

$$\Lambda(C_e) = (3 \times 10^{-4} - 5 \times 10^{-5})\ \text{m}^{-2}. \tag{19}$$

Thus, it is possible to firmly state that the main variability of $A_0$ in (13) is due to its dependence on both the wind-wave age (the quantity $U_a/c_p$, which is related to $(C_e/u_{*w})$ in (13)) and the wind speed (through $K_0 \sim \frac{U_a^3}{g}$). In order to determine the relation between the quantity $u_{*w}$ and the wind speed, it is best to use the conventional approach in which

$$u_{*w} = \left(\frac{\rho_a}{\rho_w}\right)^{1/2} u_{*a}; \quad u_{*a} = C_f^{1/2} U_a; \quad C_f = 10^{-3}; \quad \frac{\rho_a}{\rho_w} \sim 10^{-3}, \tag{20}$$

where $\rho_a$ is the air density, $u_{*a}$ is the friction velocity in the near-water atmospheric layer, $C_f$ is the resistance coefficient for the sea surface, and $U_a$ is the near-water wind speed. Then,

$$\frac{C_e}{u_{*w}} = \frac{C_e}{U_a}\left(\frac{\rho_a}{\rho_w} C_f\right)^{-1/2}. \tag{21}$$

For calculations of $A_0$ in (13), we chose the following numerical values for the constants $\alpha$ and $b$ in accordance with [1]: $\alpha = 1$ and $b = 1.0 \times 10^{-3}$, where the latter is the average value in the range $(7–13) \times 10^{-4}$, which is indicated in [1]. Thus, the quantity $\frac{b\alpha}{5}$ in (13) was taken to be

$$\frac{b\alpha}{5} \approx 0.2 \times 10^{-3}. \tag{22}$$

In view of the possible ranges of variations in $\alpha$ ($\alpha = 0.5–1.0$) and $b$, this value of $b\alpha/5$ can hardly introduce errors greater than by 2–3 times. Therefore, the expression for $A_0$ may finally be written as

$$A_0 = 0.2 \times 10^{-3} \times 10^{12} \left(\frac{C_e}{U_a}\right)^4 \Lambda(C_e) K_0. \tag{23}$$

The quantity $\Lambda(C_e)$ will be taken as the average value over the entire range of values $C_e = 2.5–6.0$ m/s in accordance with the experimental data presented in [1] (see also Fig. 5 in [5]). In this range, $\Lambda(C_e) = (2 \times 10^{-4}–5 \times 10^{-5})$, which yields the average value $1.2 \times 10^{-4}$. It is seen from Fig. 5 in [5] that, in the range $C_e = (3.0–4.5)$ m/s, the quantity $\Lambda(C_e)$ hardly varies and remains at the level of $2 \times 10^{-4}$. Thus, choosing $\Lambda(C_e) \approx 1.2 \times 10^{-4}$, we also take into account a small (but noticeable) decrease in the values of $\Lambda(C_e)$ with increasing $C_e$ (in the range $C_e \approx (4.5–6.0)$ m/s). For a more convenient comparison of the results of calculating $A_0$ according to (23) with the available data of direct measurements of $A_0$, we present the SWADE experimental dependences of $A_0$ on the wind-wave age $U_a/c_p$ [7] in Figs. 1–3. (Recall once again that the only value $\frac{\omega_g U_a}{g} = 5.0$ was used in calculations of $K_0$.) In Fig. 1, which was borrowed from [3], it is seen that the region where $\varepsilon_t(z) = \text{const}$ is fairly well defined for $\frac{u_{*w} z}{K_0} > 1.5$, and only six points near the surface show a marked tendency of increasing $\varepsilon_t(z)$ as the surface is approached. Figures 2 and 3 were constructed with these six points eliminated, so that the dependence of $A_0$ on $U_a/c_p$ was found only for those $\varepsilon_t$ values that belonged to the region of constant (in depth) values of $\varepsilon_t$. In order to compare the observational data shown in Figs. 1–3 with the results of calculations by formula (23), we have presented a table of $A_0$ values for different values of $\frac{U_a}{C_e}$. Taking into account that, as a rule, $C_e \ll c_p$, or approximately $C_e \approx (0.5–0.3)c_p$, we determined the variability of $A_0$ for the range $\frac{U_a}{C_e} = 2–6$, which appeared to correspond to the experimental conditions of SWADE [3]. In addition, because the SWADE experiment [3] was conducted under conditions when the average near-water wind speed varied in the range 8–12 m/s, we performed calculations for wind speeds of 5, 10, and 15 m/s. The final results of

Values of $\ln A_0$ for different values of $V_a/C_e$ and wind speeds $U_a$ = 5, 10, and 15 m/s

| $U_a/C_e$ | $U_a$ = 5 m/s | $U_a$ = 10 m/s | $U_a$ = 15 m/s |
|---|---|---|---|
| 1.0 | 3.36 | **5.50** | 6.71 |
| 1.2 | 2.627 | 4.767 | 5.98 |
| 1.4 | 2.013 | 4.153 | **5.36** |
| 1.6 | **1.46** | 3.603 | 4.813 |
| 1.8 | 1.01 | 3.15 | 4.36 |
| 2.0 | 0.59 | 2.73 | 3.94 |
| 2.2 | 0.19 | 2.33 | 3.54 |
| 2.4 | –0.146 | 2.00 | 3.20 |
| 2.6 | | 1.69 | 2.90 |
| 2.8 | | 1.37 | 2.58 |
| 3.0 | | 1.08 | 2.29 |
| 3.2 | | 0.85 | 2.06 |
| 3.4 | | 0.594 | 1.80 |
| 3.6 | | **0.37** | 1.58 |
| 3.8 | | 0.16 | **1.37** |
| 4.0 | | –0.06 | 1.17 |
| 4.2 | | | 0.97 |
| 4.4 | | | 0.78 |
| 4.6 | | | 0.61 |
| 4.8 | | | 0.39 |
| 5.0 | | | 0.28 |
| 5.2 | | | 0.11 |
| 5.4 | | | –0.04 |

Note: The values chosen for the constants in $C_e$ calculations in (23) are indicated in the text. The ranges of $\ln A_0$ values presented in Figs. 1–3 are separated in the table and are shown hravy numbers.

these calculations by formula (13) for $\Lambda(C_e) = 1.2 \times 10^{-4}$ m$^{-2}$2/s are given in the table and Fig. 4, and the reader can judge their agreement with the experimental data presented in Figs. 1–3. It can be seen that, for temperate wind speeds of 5 to 15 m/s, the observed values of $A_0$ are in the range of real values $\frac{U_a}{c_p} = 0.3–1.7$.

## 5. CONCLUSIONS

We have paid special attention to determining the turbulent-energy dissipation value $\varepsilon_0$ beneath breaking waves. The point is that the theory of gas transfer between the ocean and the atmosphere [14] shows that the gas transfer velocity $V_{tR}$ for $CO_2$, $O_2$, and other gases (resistance to their vertical transfer is established in the water medium rather than in the air) is described by the formula

$$V_{tR} = (\varepsilon_0 \nu)^{1/4} f(\mathrm{Pr}), \qquad (24)$$

where $\varepsilon_0$ is the characteristic value of turbulent-energy dissipation in turbulent patches that form in the course of wind-wave breaking, $\nu$ is the viscosity of air, and Pr is the Prandtl number. It follows that the gas transfer velocity, which is

$$V_{tR} = A_0^{1/4} u_{*w} \left(\frac{\nu}{K_0}\right)^{1/4} f(\mathrm{Pr}), \qquad (25)$$

in accordance with (4), not only depends on the wind speed (via $u_{*w}$ and $K_0 \sim \frac{U_a^3}{g}$) but also depends substantially on the stage of wind-wave development (through $A_0$). In view of (23), it can even be stated that the gas transfer velocity increases with wind-wave growth because $A_0^{1/4} \sim \left(\frac{U_a}{c_p}\right)^{-1}$. The data presented in [15–18] indicate that a dependence of this kind actually occurs, and we intend to devote a separate study to its description as well as to a discussion of the methods for calculating the transfer of greenhouse gases between the ocean and the atmosphere.

## REFERENCES

1. O. M. Phillips, F. L. Posner, and Y. P. Hansen, "High Range Resolution Radar Measurements of the Speed Distribution of Breaking Events in Wind-Generated Ocean Waves: Surface Impulse and Wave Energy Dissipation Rates," J. Phys. Oceanogr. **31**, 450–460 (2001).
2. S. A. Kitaigorodskii, "New Evidence for the Influence of Nonlinear Wind Wave Breaking on the Increase of Kinetic Energy Dissipation in the Upper Ocean," Dokl. Akad. Nauk **376**, 539–542 (2001).
3. S. A. Kitaigorodskii, "On the Influence of Wind Wave Breaking on the Structure of the Subsurface Oceanic Turbulence," Izv. Akad. Nauk, Fiz. Atmos. Okeana **37**, 566–576 (2001) [Izv., Atmos. Ocean. Phys. **37**, 525–536 (2001)].
4. S. A. Kitaigorodskii, "Methodological Grounds of Describing the Aerodynamic Roughness Parameter of the Sea Surface," Izv. Akad. Nauk, Fiz. Atmos. Okeana **39**, 229–334 (2003) [Izv., Atmos. Ocean. Phys. **39**, 203–207 (2003)].
5. S. A. Kitaigorodskii, "Methodological Grounds of Choosing Empirically Grounded Schemes for Modeling

Wind-Induced Waves," Izv. Akad. Nauk, Fiz. Atmos. Okeana **40**, 651–654 (2004) [Izv., Atmos. Ocean. Phys. **40**, 583–594 (2004)].

6. S. A. Kitaigorodskii, "Similarity Theory As Applied to the Upper Ocean Turbulence," Izv. Akad. Nauk, Fiz. Atmos. Okeana **34**, 430–434 (1998) [Izv., Atmos. Ocean. Phys. **34**, 385–389 (1998)].
7. S. A. Kitaigorodskii, "A Note on the Influence of Breaking Wind Waves on the Aerodynamic Roughness of the Sea Surface as Seen from Below," Tellus **46**, 681–685 (1994).
8. W. M. Drennan, M. A. Donelan, E. A. Terray, and K. B. Katsaros, "Oceanic Turbulence Dissipation Measurements in SWADE," J. Phys. Oceanogr. **26**, 808–815 (1996).
9. J. H. Duncan, "An Experimental Investigation of Breaking Waves Produced by a Towed Hydrofoil," Proc. Roy. Soc. London A, **377**, 331–348 (1981).
10. W. K. Melville, "Energy Dissipation by Breaking Waves," J. Phys. OceanÓgr. **24**, 2011–2049 (1994).
11. O. M. Phillips, "Spectral and Statistical Properties of the Equilibrium Range in Wind Generated Gravity Waves," J. Fluid Mech. **156**, 505–535 (1985).
12. S. A. Kitaigorodskii, "Effect of Breaking of Wind-Generated Waves on the Local Atmosphere–Ocean Interaction," Izv. Akad. Nauk, Fiz. Atmos. Okeana **33**, 828–836 (1997) [Izv., Atmos. Ocean. Phys. **33**, 767–774 (1997)].
13. S. A. Kitaigorodskii, *Dissipative Range in the Spectrum of Wind Waves: Bibliography* (Meteorologiya i Gidrologiya, Moscow, 2002) [in Russian].
14. S. A. Kitaigorodskii, "On the Fluid Dynamical Theory of the Turbulent Gas Transfer across an Air–Sea Interface in the Presence of Breaking Wind Waves," J. Phys. Oceanogr. **14**, 960–972 (1984).
15. *Gas Transfer at Water Surfaces*, Ed. by M. A. Donelan et al. (American Geophysical Union, Washington, 2002).
16. D. Zhao and Y. Toba, "Dependence of Whitecap Coverage on Wind—Wave Properties," J. Oceanogr. (Oceanogr. Soc. Jpn.) **57**, 603–616 (2001).
17. D. Zhao, Y. Toba, Y. Suzuki, et al., "Effect of Wind Waves on Air—Sea Gas Exchange. Proposal of on Overall $CO_2$ Transfer Velocity Formula as a Function of Breaking Wave Parameter," in *Proceedings of Sixth International Carbon Dioxide Conference* (2001).
18. D. Zhao, Y. Toba, Y. Suzuki, and S. Komori, "Effect of Wind Waves on Air–Sea Gas Exchange: Proposal of an Overall $CO_2$ Transfer Velocity Formula as a Function of Breaking Wave Parameter," Tellus B **55**, 478–487 (2003).